

PAPER M

DIFFRACTION TOMOGRAPHY FOR INHOMOGENEITIES IN A LAYERED BACKGROUND MEDIUM (CONT.)

Jerry M. Harris and Guan Y. Wang

ABSTRACT

A Fourier back-propagation inversion for a stratified background and point sources is developed by using the normal mode solution to the acoustic wave equation. The spectrum of an object function describing the heterogeneity is decomposed into contributions from different layers and then the selection rule is applied to the spectrum of the individual layers. This method differs from its counterpart for a uniform host medium by a propagation matrix filter that reduces to unity as the stratification degenerates to be uniform. Since the theory deals directly with point sources in a cylindrical background medium the algorithm does not require 2.5-D correction when applied to field data as usually performed in previously published diffraction tomography algorithms.

INTRODUCTION

The general theory of diffraction indicates, at least in principle, that diffraction tomography has the potential to achieve maximum spatial resolution and minimum image distortion for crosswell seismic data (Devaney, 1984), (Harris, 1987) and (Wu et. al., 1987). However, in its conventional form, diffraction tomography is used to image a weak inhomogeneity of arbitrary shape embedded in a uniform medium. Its application is successful only if the inhomogeneities represent small deviations from the background and if the correlation lengths of these deviations are large compared to a wavelength. In situations involving oil and gas reservoirs to which we hope to apply the method, these conditions are usually not satisfied.

However, small changes of velocities superposed on large stratified variations is of great interest to reservoir imaging. Various scenarios based on a layered background model

have been studied, either in data space or model space: Devaney & Zhang (1991) used slant stacks to preprocess and map tomographic data with the layered background into an equivalent constant reference background data set and then applied a conventional diffraction tomography algorithm to the preprocessed data. Huang (1992) applied WKBJ solution for the Green's function to simplify the propagator and extended the constant background back-propagation algorithm to allow for smooth variations in depth. Pai (1990) and Dickens (1992) decomposed the wave fields of the layered host medium by using vertical eigenstates and then numerically reformulated the problem.

We present a new formulation of diffraction tomography to account for the effects of the layered host medium and incident fields radiated by point sources. The formulation is based on the characteristics of normal modes and the coefficients of their excitation in a N-layer medium. The solution from the superposition of normal modes is used to construct a Green's function and therefore, the scattered fields generated by perturbations of velocity in the layers. The Green's function of the layered background enables one to ensure small contrast between the inhomogeneity to be imaged and the host velocity in each layer. The resulting scattered field is always weak and can be neglected relative to the background field when estimating the total fields. This approximation is locally valid and is called the "distorted Born" approximation. To solve the imaging problem, we decompose the Fourier spectrum of the heterogeneity into contributions from different layers by taking advantage of the linear superposition property of the Fourier transform. We then apply the selection rule, in which the scattering field in diffraction space is related to the Fourier transform of the heterogeneity, to individual layers. It turns out that the algorithm for layered medium is similar to the one for homogeneous background except that an additional filter is involved which results from the propagation matrix of the layer parameters of the medium. An imaging algorithm based on this formulation is applied to synthetic and field data. Results demonstrate that an inversion with spatial resolution of the order of a wavelength can be achieved for crosswell seismic data.

ACOUSTIC WAVE EQUATION IN THE LAYERED MEDIUM

For the crosswell geometry, we select a cylindrical coordinate system that is oriented so that the positive z-axis is vertical downward. The background medium is assumed to be isotropic and stratified in layers with constant velocity and density. Under these assumptions, the acoustic equation can be written as:

$$\frac{\partial^2 G}{\partial r^2} + \frac{1}{r} \frac{\partial^2 G}{\partial z^2} - \frac{1}{r(z)} \frac{dr}{dz} \frac{\partial G}{\partial z} + k^2(z)G = -\frac{1}{2\pi r} \delta(z - z_s) \delta(r) \quad (1)$$

where $\rho(z) = \rho_l$, $k(z) = \omega/v_l$, and G is a Green's function. Since the boundary surface coincides with coordinate surfaces and the property of the background medium is assumed to vary only with depth, we can apply the method of separation of variables. The solution can be written as a superposition of normal modes $\psi_n(z)$

$$G(r, z) = \sum_{n=0}^{\infty} \phi_n(r) \psi_n(z) \quad (2)$$

Substituting this expansion into the Eqn (1) we get

$$\frac{d^2 \phi_m}{dr^2} + \frac{1}{r} \frac{d\phi_m}{dr} + k_m^2 \phi_m = -\frac{\psi_m^{(l)}(z_s)}{2\pi r \rho_l} \delta(r) \quad (3)$$

where l is for l^{th} layer. The solution of Eqn (3) is the Hankel function of the first kind and zero order. Therefore, the Green's function for the acoustic wave equation for any depth z and offset r in the layered medium can be written as

$$G_l(r, z) = \sum_m^{\infty} \frac{\psi_m^{(l)}(z_s^{(l)})}{\rho_l} \psi_m^{(l)}(z) H_0^{(1)}(k_m r) \quad (4)$$

Using this modal superposition, the scattered field generated by a heterogeneity embedded in the medium can be constructed.

SINGER SCATTERING IN THE DISTORTED BORN APPROXIMATION

We determine the forward scattered fields using the Green's function of Eqn (4). We can always choose an appropriate layered background to ensure the velocity contrast between the inhomogeneity and the host medium remains small. Therefore, the scattered fields caused by the contrast are small compared to the distorted incident field. With the application of Green's theorem and distorted Born approximation, the scattered field u^{sc} can be written as the superposition of integrals

$$u^{sc}(r_s, z_s, r_g, z_g) = - \sum_l \int_{v_l} k_l^2 O_l(r, z) G_s(r, z) G_g(r, z) dv \quad (5)$$

where $O_l(r, z) = 1 - v_l^2/v^2$ is the objective function describing the heterogeneity $k_l = \omega/v_l$, G_s and G_g are Green's functions respect to source and receiver. Note that Eqn (5) can always be decomposed into the propagating and non-propagating modes. Since we are interested only in propagating fields, Eqn (5) can be written as

$$u^{sc}(r_s, z_s, r_g, z_g) = - \sum_l \sum_{n,m} \int_{v_l} k_l^2 O_l(r, z) \{A_n^l A_m^l e^{i(g_n + g_m)z + i(g_n z_s + g_m z_g)} B_n^l B_m^l e^{-i(g_n + g_m)z - i(g_n z_s + g_m z_g)}\} H_0^{(1)}(k_n |r_s - r|) H_0^{(1)}(k_m |r - r_g|) dv \quad (6)$$

where the A 's and B 's are propagation matrices of the layered background medium.

FOURIER BACK-PROPAGATION IN THE LAYERED BACKGROUND

Taking the discrete Fourier transform of the forward scattered field along the depth of the source well and the receiver well, we get

$$u^{sc}(r_s, r_g; k_s, k_g) = \sum_l \left\{ \int_{v_l} k_l^2 O_l(r, z) D(k_s, k_g) \times e^{i(k_s + k_g)z} H_0^{(1)}(\gamma_s |r_s - r|) H_0^{(1)}(\gamma_g |r - r_g|) dr dz \right\} \quad (7)$$

where $D(k_s, k_g) = (A_{k_s}^{(l)} A_{k_g}^{(l)})^2 + (B_{k_s}^{(l)} B_{k_g}^{(l)})^2$. Applying the localization principle (Babic, 1972), we can replace the Hankel functions in Eqn (7) by their first order Taylor expansions in the neighborhood of the observation point r . The physical meaning of the expansion is that a cylindrical wave represented by Hankel functions can be replaced, locally by a plane wave whose direction of propagation, amplitude and phase all change from point to point. The integrals on the right side of the Eqn (7) then can be arranged into the Fourier transforms of the inhomogeneity function O_l . Utilizing the linear property of the Fourier transform, we

can decompose the spectrum of the scattering field into contributions by inhomogeneities from different layers, i.e.

$$O_i(K_r, K_z) = [u^{sc}(r_s, r_g; k_s, k_g) * \sin c(K_z z_i)] W \quad (8)$$

where

$$W = \frac{r_g \gamma_s^{(l)} \gamma_g^{(l)} e^{-i\gamma_g^{(l)} r_g + i\gamma_s^{(l)} r_s}}{D(k_s, k_g) k_i^2} \frac{e^{i\gamma_g^{(l)} r_g - i\gamma_s^{(l)} r_s}}{r_g \gamma_s^{(l)} \gamma_g^{(l)}}$$

where $K_z = k_s + k_g$ and $K_r = \gamma_s^{(l)} - \gamma_g^{(l)} = \sqrt{k_1^2 - k_s^2} - \sqrt{k_1^2 - k_g^2}$. In the image space, the objection function can be evaluated as

$$O_i(r, z) = F^{-1}\{O_i(K_r, K_z) |J|\}(k_s, k_g) \quad (9)$$

where J is Jacobean transform matrix, and operator F^{-1} is inverse Fourier transform in which k_s, k_g are independent variables.

RECONSTRUCTION WITH SYNTHETIC DATA

We will illustrate the new method with two synthetic examples. For the first example, the wave field for a 2-D heterogeneity is calculated with a finite difference method and then transformed into the frequency domain. The responses in the range of 1100-1300 Hz are averaged. The model and reconstructed images are shown in Figure 1. From the reconstruction we can see that the boundary of the inhomogeneity is imaged correctly but blurred in the horizontal direction due to poor coverage of the crosswell geometry. This distortion is attributed to the effects of limited aperture, the source function and the incompatibility between the 2-D line source synthetic data and the inversion theory for point sources.

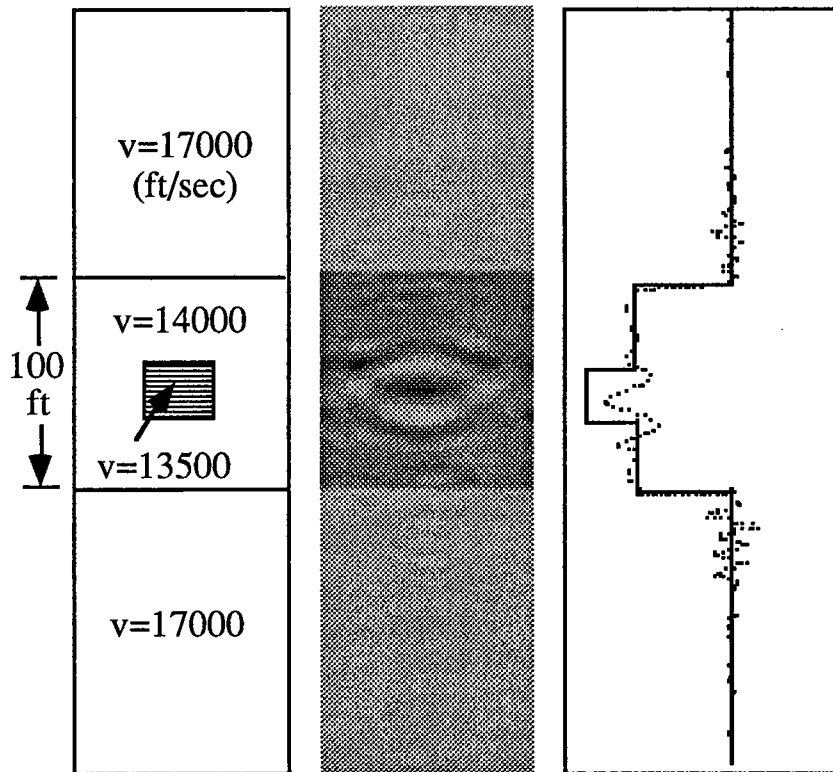


Fig 1. (a) the model used to generating synthetic data, (b) reconstruction from the synthetic data, and (c) the cross sections along the depth. The solid line is from the model and the dash line from the reconstruction

For the second synthetic example, the model consists of several thin beds embedded in a four layer background medium. The synthetic data are calculated directly in the frequency domain with a point source. The image, shown in Figure 2, provides an excellent reconstruction of the small perturbations in the model, especially the location of the thin beds, see Figure 2.

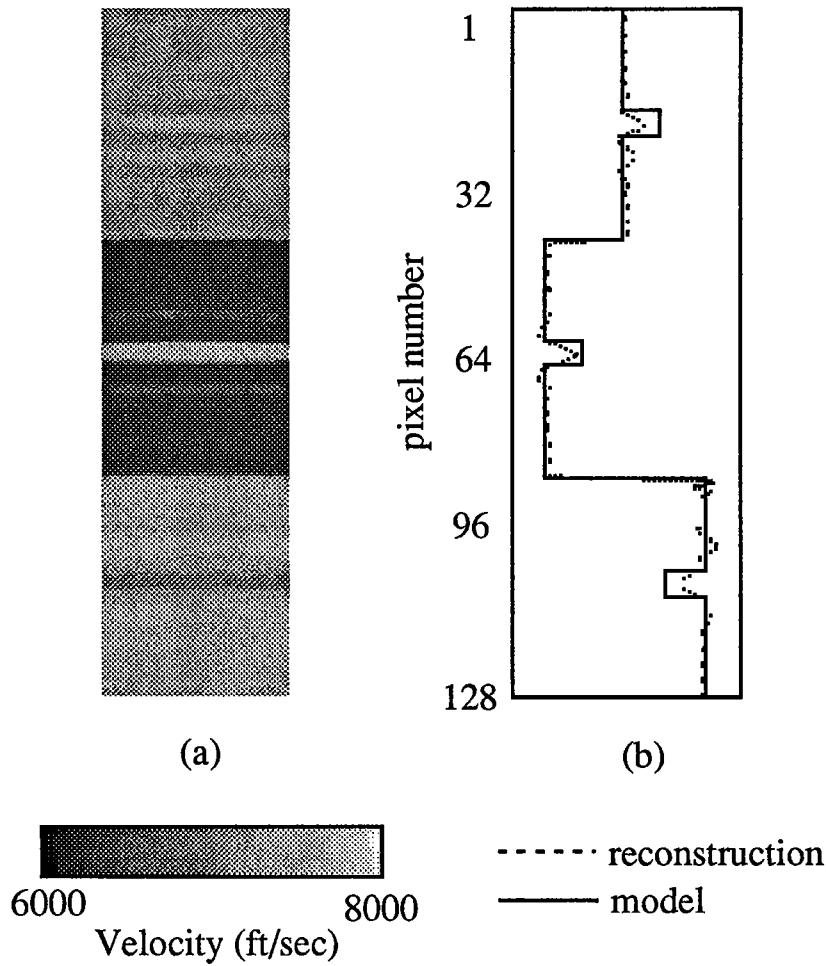


Fig. 2. 1-D synthetic data inversion: (a) reconstructed image from a layered background, (b) cross sections along depth. The solid line for the model and dash line for image

RECONSTRUCTION WITH FIELD DATA

We apply the algorithm to the field data from west Texas. A traveltime tomography of the field data (Figure 4a, Van Schaack, 1992) is used to create a 1-D background model for

the inversion. Amplitudes of the field data are normalized at a chosen receiver position to reduce the effects of the source function and coupling. The parameters used in the calculation are indicated in Table 1.

Table 1.

| | |
|---------------------------|-----------------|
| Number of source/receiver | 128 |
| Frequency | 1100 to 1700 Hz |
| Well separation | 184 ft |
| Well line depth | 320 ft |
| source/receiver sampling | 2.5 ft |

The images are reconstructed with the field data at frequencies of 1100, 1300, 1500 and 1700 Hz respectively. Internal structure of the reservoir located between 1850 to 1950 ft is identifiable in every reconstruction of Figure 3. Although the reservoir zone can be seen in the tomogram, its internal structure is not resolved by traveltime tomography. This is not surprising, because in essence, transmission traveltime tomography reconstructs the low frequency components of the inhomogeneities while the diffraction tomography recovers the higher spatial frequencies.

We stacked the images of Figure 3 to form the result shown in Figure 4. Since simple stacking of the images from different frequencies is not coherent for limited apertures, the resolution is reduced. Stacking does, however, offer the advantages of removing unsightly aperture distortions. It would be a good idea to stack coherently to enhance desired features and incoherently to get rid of unwanted distortions. But a coherent multi-frequency stacking may involve data stretching and interpolation in wave number domain which generally is difficult to apply to the situation of inhomogeneous background. But a coherent multi-frequency stacking may involve data stretching and interpolation in wave number domain which generally is difficult to apply to the situation of inhomogeneous background.

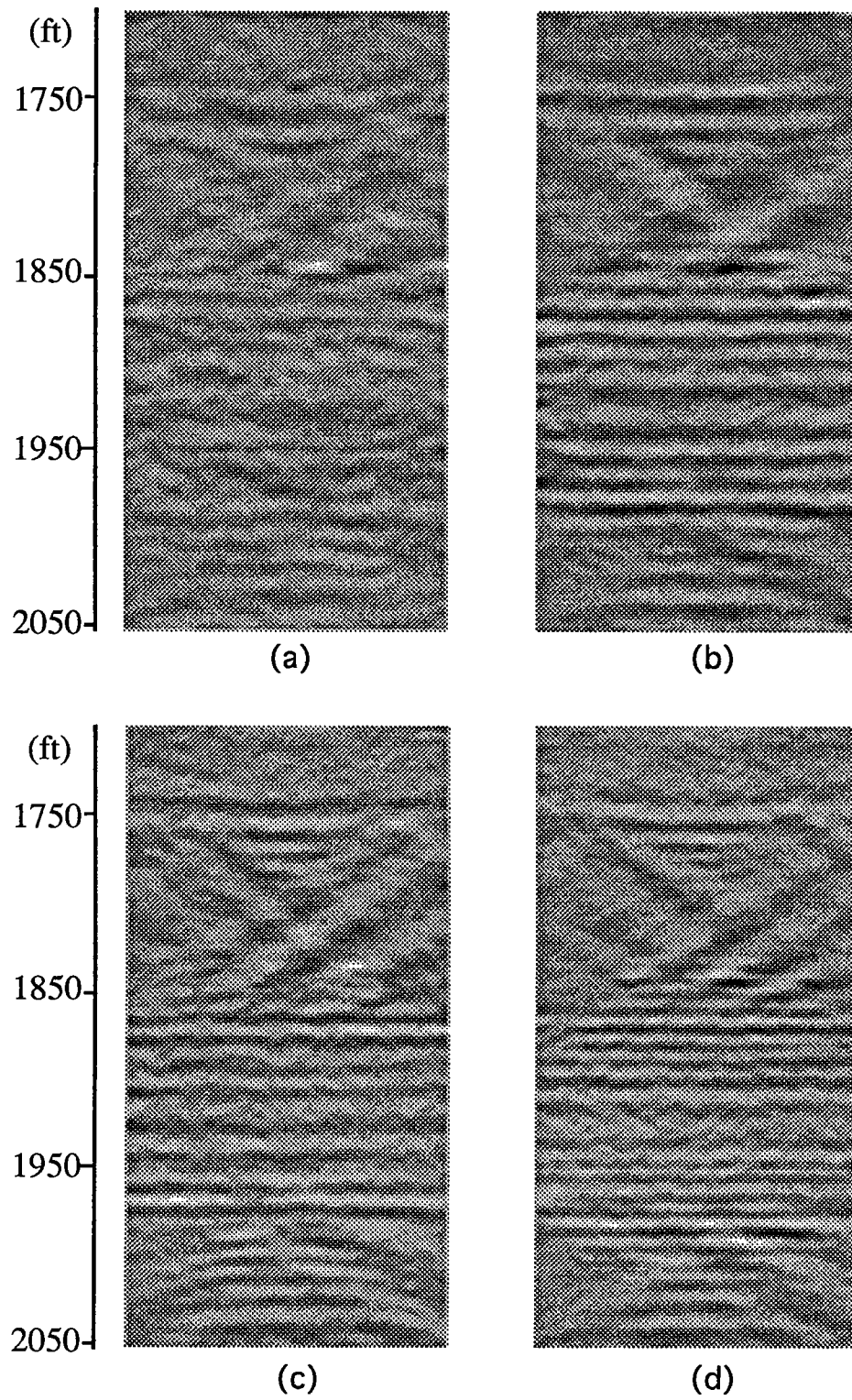


Fig 3 Field data inversions. (a), (b), (c) and (d) are reconstructed images of the object function at frequency equal to 1100, 1300, 1500 and 1700 Hz respectively.

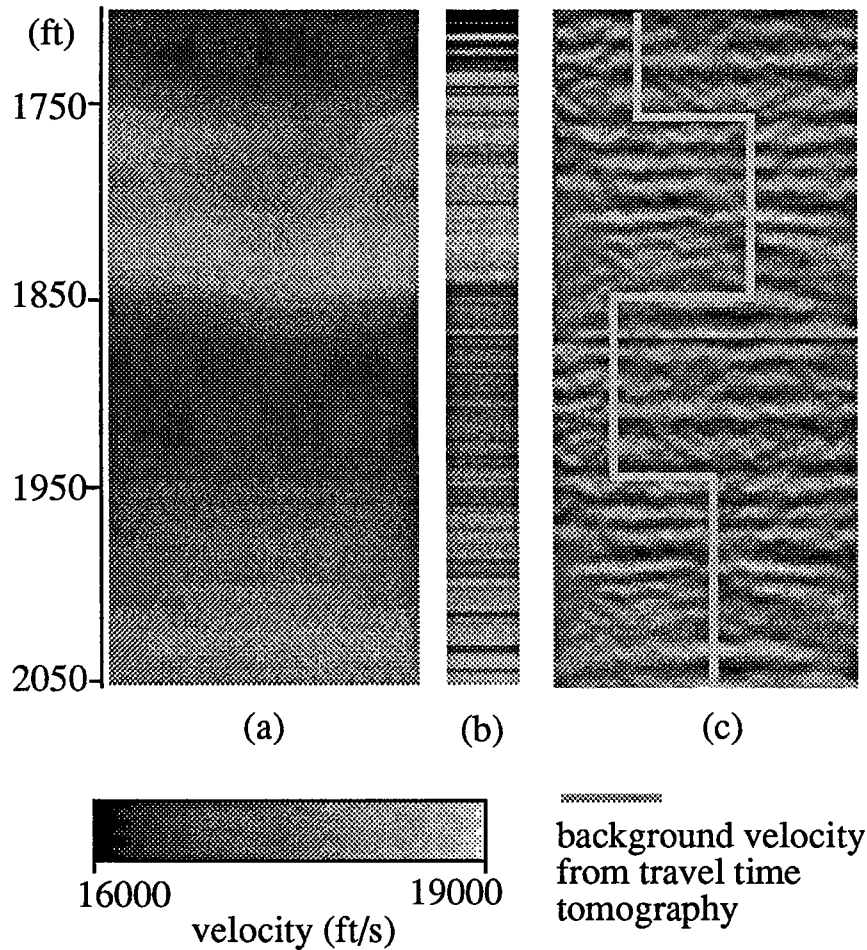


Fig. 4 Field data inversion: (a) travelttime tomogram, (b) the sonic log and (c) the objection function image with white line representing layered background.

RESOLUTION AND DISTORTION OF THE IMAGE

The resolution of the diffraction constructed image depends on the coverage in wave number domain, and therefore on the length of the source/receiver apertures and the aspect ratio of the apertures to well separation (Fig. 12). Larger aspect ratio provided more angular coverage and hence better resolution. Generally, the maximum horizontal wave number is smaller than vertical wave number, resulting in poorer resolution in horizontal direction. For the examples discussed here, the wave length of the incident wave is about 10 ft. The spatial

sampling interval of the measurement and the pixel spacing of the image are both chosen to be 2.5 ft to fully utilize the resolution provided in the data.

We analyze the resolution of the reconstructed image from following two aspects: The resolution limitation of the algorithm and the effects of limited angular coverage including short source/receiver arrays and relatively low frequency. In an ideal situation in which the source/receiver lines tend to infinity, the maximum vertical wave number is $\max\{K_z\}=2\pi/\Delta$ and the maximum horizontal wave number $\max(K_x)=\lambda$, where Δ is 2.5 and equal to $\lambda/4$. Therefore, the best resolution of the image would be $\lambda/4$ in vertical direction and λ in horizontal direction. Due to the limited aperture and relatively low frequency, the wave numbers in both vertical and horizontal directions can not reach these maximum values and the reconstructed image is blurred. In other words, the resolution of the reconstructed image is reduced. This process can be understood in terms of the convolution between the aperture sinc function and the image, i.e. $\hat{o}(r) = \text{sinc}(Lr) * o(r)$ where $\hat{o}(r)$ is the estimated image, L is source/receiver apertures which is limited, and $O(r)$ is the ideal image with infinite long aperture (Zhou, 1990). Taking consideration both of resolution limits and the distortion effects of limited aperture, the actual resolution of the image can be estimated as approximately 0.5λ and 1.5λ in vertical and horizontal direction respectively.

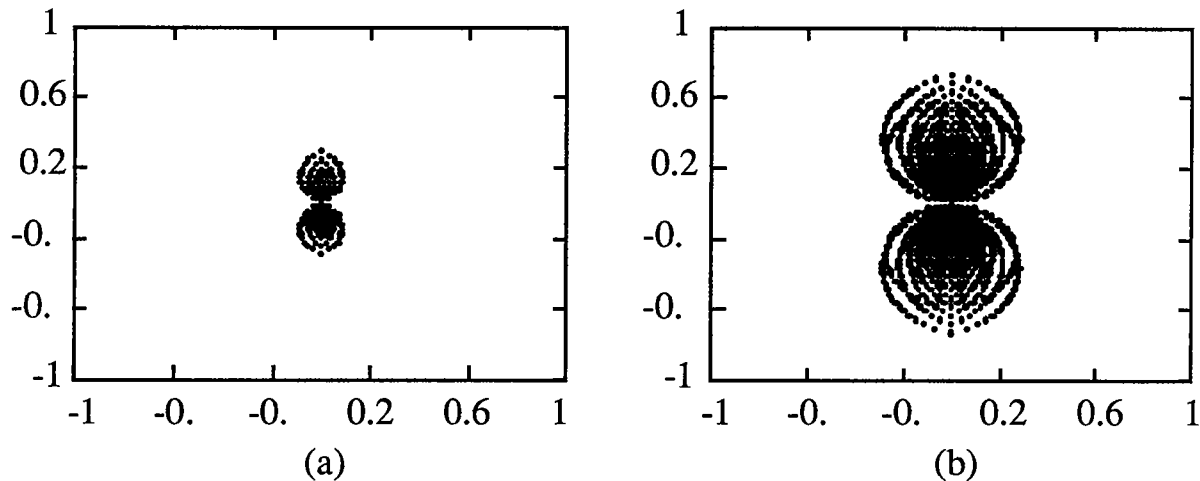


Fig. 5 K-space coverage of limited aperture in cross-well geometry:
 (a) the single frequency and (b) the multi-frequency coverage

CONCLUSIONS

A diffraction tomography algorithm has been shown to be effective in crosswell imaging with both synthetic and field data. Effectiveness of the method is achieved by properly choosing a stratified background medium to maintain the validity of the Born (or Rytov) approximation, thereby allowing decomposition of the heterogeneity spectrum into contributions from individual layers. Due to the fact that this algorithm directly deals with point sources, no 2.5-D correction is needed to be applied to the field data. The ability of the algorithm to provide high resolution images depends on the extent of source and receiver apertures of the measurement. However, this limitation exists for all imaging methods not just for crosswell diffraction tomography. If high frequency data are available, the inhomogeneities can be well recovered by this diffraction tomography method. We hope to extend this algorithm to be able to use multi-frequency data to increase the wave number spectra and therefore to improve resolution.

REFERENCE

- Devaney A. J., Zhang D., 1991, Geophysical diffraction tomography in a layered background, *Wave Motion*, 14, 243-265
- Devaney, A. J., 1984, Geophysical diffraction tomography, *IEEE Trans. Geosci. remote Sensing*, Vol. GE-22, no. 1, pp. 3-13
- Dickens T. A., 1992, Study of diffraction tomography for layered backgrounds: SEG expanded abstract
- Harris J. M., 1987, Diffraction tomography with arrays of discrete sources and receivers: *IEEE trans. Geosci. and Remote Sensing*, 25(4), 448-455.
- Huan, L., Wu, R., 1992, Multifrequency backscattering tomography: extension to the case of vertical varying background, SEG expand abstract
- Pai, D. M., 1990, Crosshole seismic using vertical eigenstates: *Geophysics*, 55(7), 815-820.
- Van Schaack M., Harris J. M. Rector III J. W., & Lazaratos S. K., 1992, High resolution Crosswell imaging of a West Texas carbonate reservoir, SEG, expanded abstract
- Wu, R. and Toksoz, M. N. 1987, Diffraction tomography and multi-source holography applied to seismic imaging, *Geophysics*, 52, 11-25
- Zhou, Q. 1990, Audio-frequency electromagnetic tomography for reservoir evaluation: Ph.D thesis, UC Berkeley